

CHAPTER 40

**MORPHOLOGY FROM IMAGERY: DETECTING AND MEASURING THE
DENSITY OF URBAN LAND USE**

(TV Mesev, P Longley M Batty and Y Xie)

Environment and Planning A, 1995, 27, 759-780

Morphology from imagery: detecting and measuring the density of urban land use

T V Mesev, P A Longley

Department of Geography, University of Bristol, University Road, Bristol BS8 1SS, England

M Batty, Y Xie

National Center for Geographic Information and Analysis, State University of New York, Wilkeson Quad, Buffalo, NY 14261-0023, USA

Received 15 January 1994; in revised form 20 April 1994

Abstract. Defining urban morphology in terms of the shape and density of urban land use has hitherto depended upon the informed yet subjective recognition of patterns consistent with spatial theory. In this paper we exploit the potential of urban image analysis from remotely sensed data to detect, then measure, various elements of urban form and its land use, thus providing a basis for consistent definition and thence comparison. First, we introduce methods for classifying urban areas and individual land uses from remotely sensed images by using conventional maximum likelihood discriminators which utilize the spectral densities associated with different elements of the image. As a benchmark to our classifications, we use smoothed UK Population Census data. From the analysis we then extract various definitions of the urban area and its distinct land uses which we represent in terms of binary surfaces arrayed on fine grids with resolutions of approximately 20 m and 30 m. These images form surfaces which reveal both the shape of land use and its density in terms of the amount of urban space filled, and these provide the data for subsequent density analysis. This analysis is based upon fractal theory in which densities of occupancy at different distances from fixed points are modeled by means of power functions. We illustrate this for land use in Bristol, England, extracted from Landsat TM-5 and SPOT HRV images and dimensioned from population census data for 1981 and 1991. We provide for the first time, not only fractal measurements of the density of different land uses but measures of the temporal change in these densities.

1 Measuring urban morphology

Whatever approach to urban analysis is taken, cities are usually visualized at some stage in terms of their geometric form. Urban economics, transportation, and social structure are predicated in spatial terms, and thus the effects of such theory are often articulated through geometric notions involving the shape of urban land use and the manner in which it spreads. Shape and density measure the way in which urban space is filled and are thus key elements in the definition of morphology. Until recently, it has been difficult to link the geometric form of real cities to formal theories explaining densities, and thus urban economic theory, for example, has evolved within highly idealized geometries which bear little relation to real spatial patterns.

The development of fractal geometry, however, which is in essence a geometry of the irregular, has clear relevance to spatial systems such as cities. The rudiments of a fractal theory of cities now exists which has the potential to synthesize many ideas from location theory with spatial form (Batty and Longley, 1994; Frankhauser, 1994). The notion that cities are self-similar in their functions has been writ large in urban theory for over a century, and is manifest in terms of relations such as the rank-size rule, hierarchical differentiation of service centers as in central place theory, transportation hierarchies and modes, and in the area and importance of different orders of hinterland (Arlinghaus, 1985; 1993). All these relations which form the cornerstones of urban geography can be described and modeled by using

power laws which are fractal. What this new geometry is beginning to do is to tie all these notions explicitly together in a geometry of the irregular, a geometry of the real world (Mandelbrot, 1983).

We take this fractal theory as our starting point and, in this paper, we use its simplest elements, which involve the measurement of shape and density. Our purpose here, however, is not to extend this theory very far but to concentrate on the equally important problem of detecting the appropriate shape and density of urban areas and the land uses which occupy them. Hitherto, most characterizations of urban land use have depended upon some visual inspection of spatial patterns and the identification of visual distinctions which serve to reinforce functional differences. Such classification is often informed by statistical analysis, but methods for controlling the consistency of such definitions between different case studies are lacking, and thus comparative analysis is limited.

Measurement, of course, prescribes analysis, and it is only as improved data sets become available and methods of representing urban phenomena become more transparent that morphological analysis becomes more tractable. In our own previous work (Batty and Longley, 1994; Longley and Batty, 1989a; 1989b) we have been aware that the definitions of 'urbanity' adopted for particular administrative purposes are not usually the most appropriate to more general measurement and analysis. Yet issues of confidentiality and aggregation dictated that socioeconomic data are rarely available for disaggregate study at finer resolutions.

Where models of socioeconomic data have been devised to interpolate continuous surfaces about point information (Martin, 1991), estimates are not accurate at any scale finer than around a 200 m resolution, and there is the concern that measurement of urban form in fact represents the assumptions in the modeling procedure, rather than the underlying distributions of individuals, buildings, and land uses which it is intended to detect. With the development of remotely sensed data, however, the prospect exists for both finer resolution and consistent classification of urban areas and land use across universally available data. This is the task we will address here, showing how the data which are derived can be interpreted by means of fractal theory.

In this paper we are thus concerned with the detection, then measurement, of urban morphologies from remotely sensed imagery. We will begin with methods for the generation of distinct land uses from such images, outlining the conventional technique of discrimination based on maximum likelihood estimators applied to the spectral bands which define such images. We augment this method by using small area census statistics from the UK Population Census to ground the interpretations we make in an independent data source, and from the resulting analysis we define discrete categories of land use for each pixel in the image. The resulting surfaces show the presence or absence of a particular land use in each cell, and it is these that are then measured in terms of their shape and density by means of fractal methods.

Here we use two broad approaches to measuring density. First, we consider the absolute amount of space within the total available which is filled by a given land use and, second, we consider the rate at which space is filled with respect to distance from some central point in the city [usually the central business district or (CBD)]. Both these methods yield various parameters, the most significant of which is the fractal dimension. However, because these methods yield different estimates, we introduce a new method which is based upon elements of each. We also test the sensitivity of these methods to reductions in the size of the images over which the analysis takes place.

The data for which we develop these applications are derived from the Landsat TM-5 image taken in April 1984 and from the SPOT HRV image taken in June 1988 for the urban area of Bristol, England. From these images, together with socioeconomic data from the 1981 and 1991 Population Censuses, different types of land use are extracted, and these form the surfaces which are then subject to fractal analysis. Four distinct components of land use can be identified from the 1981 data, eight from the 1991, and this enables some comparison, through fractal theory, of urban form in terms of individual land-use patterns. Temporal comparisons are also made, with the emphasis on comparative analysis demonstrating how such analysis can be made routine by use of remotely sensed data. We conclude the paper with some comments on the potential for using remotely sensed data for extensive comparative analysis of urban morphologies, a potential which has not been realizable hitherto.

2 Extracting land-use patterns from remotely sensed data

Standard methods for classifying remotely sensed data exist within proprietary software image analysis packages, and here we have used the most commonly used commercial per-pixel classifier, the maximum likelihood classifier based on Bayesian principles. The version we have chosen is implemented in the *Imagine* Version 8.0.2 package from ERDAS Inc., Atlanta, GA. This software computes the likelihood of a pixel belonging to any class, with the spectral categories of the image represented by Gaussian probability density functions described by associated mean vector and covariance matrices. Readers who are unfamiliar with these methods and the process are referred to any of the standard works, such as Strahler (1980). The maximum likelihood discriminant function, F_{ik} , is given as

$$F_{ik} = \frac{1}{(2\pi)^{n/2} |C_k|^{1/2}} \exp\left[-\frac{1}{2}(X_i - M_k)^T C_k^{-1} (X_i - M_k)\right], \quad (1)$$

where F_{ik} is the probability of pixel i belonging to class k ; n is the number of spectral bands; X_i is the $1 \times n$ pixel vector of spectral band values for each pixel i , where $i = 1, 2, \dots, N$; M_k is the $1 \times n$ mean vector for class k over all bands; and C_k is the $n \times n$ variance-covariance matrix for class k over all bands. M_k and C_k are based on those subsets of observations of pixels in the image that represent 'training samples' that the user identifies as being representative of each class k .

Given these parameters, it is possible to compute the statistical probability of a given pixel value being a member of a particular spectral class assuming equal class prior probabilities. Parametric classifiers such as this take into account not only the marginal properties of the data sets but also their internal relationships through the standardization on the inverse of the variance-covariance matrix of each class. This is one of the prime reasons for the great robustness of the technique as well as for its relative insensitivity to distributional anomalies. If the spectral distributions for each class deviate greatly from the normal, the procedure identifies poor performances, and if no information about the actual dimension of the group is available, areal estimates tend to be highly inaccurate (Maselli et al, 1992). The problems encountered with the conventional maximum likelihood classifier have been, to a certain extent, circumvented by nonparametric algorithms, such as the one developed by Skidmore and Turner (1988), who documented a 14%–16% improvement in overall accuracy. Their decision rule lies on the extraction of class probabilities from the gray-level frequency histograms. In this way, all the information about the class probability distribution is extracted from the analysis of

training samples, with modifications intended to preserve the areal estimates of each land-cover type.

In our applications, we have avoided the equal probability assumption by incorporating as prior probabilities knowledge from outside the spectral domain (Mesev, 1992). Prior probabilities describe how likely a class is to occur in the population of observations. They can simply be seen as estimates of the proportion of the pixels which fall into a particular class. Formally, this is the conditional probability, $P_{k|X_i, V_j}$, of spectral class k given pixel vector X_i and some ancillary variable V_j . This forms the basis of a modified decision rule, assigning the i th observation to that class k which has the highest probability of occurrence, given the multispectral dimension vector X_i (which has been observed) and ancillary variable V_j . The probability in equation (1) can thus be modified as P_{ik} with respect to these priors,

$$P_{ik} = \frac{F_{ik} P_{k|X_i, V_j}}{\sum_w F_{iw} P_{w|X_i, V_j}} \quad (2)$$

The numerator shows how the joint prior probabilities of the spectral and ancillary variable are incorporated into the maximum likelihood estimator, F_{ik} , with the denominator ensuring that all conditional probabilities sum to 1.

Classification of urban images is common within the remote-sensing literature, although the purpose of most such exercises is the differentiation between broad land-use categories rather than the differentiation of land-use types within the urban mosaic. The process of classifying an image by means of any of the standard techniques requires the user to identify in advance the number of distinct classes into which the image is to be partitioned, in this case land-use categories. To this end, we adapt established methods based upon equation (1) by defining urban areas of the image which show clusters of like spectral values as 'training samples'; these are used in an iterative process of classification of the image into relevant classes and in the computation of the appropriate likelihood statistics. The process is, of course, intuitive to a degree but it is aided by the variance-covariance analysis, and, in this case, we have used socioeconomic data from the Population Censuses to inform the process.

To this end, we have used the surface smoothing technique developed by Bracken and Martin (1989). When applied to socioeconomic data based on irregular zonal units, this method transforms the data to regular units at finer levels of spatial disaggregation (see also the approaches of Langford et al, 1991; Sadler and Barnsley, 1990). In these applications, socioeconomic data recorded in Population Census enumeration district (EDs) are spread to a finer grid. Data in each ED are associated with their appropriate centroids and are distributed spatially (according to assumptions of distance-decay) by centering, in turn, a moving window (kernel) over the cells containing each centroid. The distance-decay model is then used to compute the probability of each local (within-window) cell containing a proportion of the count. For any cell j , the variable V_j is allocated as

$$V_j = \sum_{m \in C} V_m W_{jm}, \quad (3)$$

where V_j is the estimated value in the j th cell of the output surface; V_m is the value of the variable assigned to the m th centroid (where C is the total number of centroids in the model area) and W_{jm} is a unique weighting of cell j relative to centroid m (based on the distance-decay assumptions). This method enables data on irregular surfaces to be disaggregated to spatial units which reduce the dependence of density

on the geographic tessellation used (Openshaw, 1984). In these applications, the surfaces are in a raster format with a resolution of $200\text{ m} \times 200\text{ m}$.

The process of generating land-use classes is informed by the surfaces generated from census data in two ways: by directing the training sample process and by determining the areal estimates for each class (Mesev, 1993). First, samples of classes are needed for all supervised image classifications. These are usually spectrally homogeneous areas of the image that represent a distinct category. Urban-rural distinctions are relatively straightforward. Artificial structures are physically more solid and smoother than vegetation or soil. As a result, urban areas tend to reflect higher proportions of their incident energy than their rural counterparts.

The spectral recognition of housing types is primarily based upon the amount of building materials per pixel, where, for example, detached housing represents the lowest ratio of materials to nonbuilding materials (vegetation, soil, water, etc). Additional information is essential to define the most appropriate breaks in the somewhat continuous multispectral data that represent built-up land, and this is where the census data are used. The surface model can display areas with high probabilities of occurrence of concentrations of particular census variables. For example, ED cells with large relative counts of, say, terraced housing can be used to direct the analyst towards that part of the image for the selection of a training sample to be labeled 'terraced housing'. For this to be possible, both the satellite image and the surface model need to be in very close spatial agreement. We illustrate this in the empirical work which follows.

Second, the deterministic probabilities of census variables are in effect the prior probabilities. As described, they can weight each training sample within the maximum likelihood classifier. For example, if the census indicates that terraced housing represents 39% of the residential land cover of a scene, then this should be incorporated into the maximum likelihood algorithm as a prior probability of 0.39. The effect is to preserve the areal approximations of the terraced-housing category. We will show how these various elements are used in the analysis of the Bristol images when we broach the empirical work introduced below where we indicate how probabilities are transformed to distinct (binary) land-use categories.

3 Density and fractal dimension

There are a multitude of geometric measures of morphology which could be applied to cities, but, as we noted in the introduction, we concentrate here upon the spread of cities in terms of their density, using ideas from fractal geometry which relate the conventional theory of urban density to the irregularity and self-similarity of urban shapes (Batty and Longley, 1994). Urban systems, particularly in the developed world, display clear patterns of density with respect to their historic development, despite changes in overall densities and massive shifts in population over the last century. Even where development no longer focuses upon this core-edge cities as they are called in North America—density still declines with distance from the original seed of development because of inertia in the built form and the fact that rent per unit of space is always higher in denser areas.

The traditional model originates from Clark (1951) and is based on the definition of population density $p(R)$ at distance R from the core (or CBD) as a negative exponential function of that distance R . Then,

$$p(R) = \lambda \exp(-\lambda R), \quad (4)$$

where λ is a friction-of-distance parameter, or elasticity, controlling the spread or density. In fact, we argue elsewhere (Batty and Kim, 1992) that this model, although originally predicated as a better alternative to the Pareto or inverse power law which appears extensively in social physics, is flawed: its parameter is scale dependent whereas urban systems manifest a degree of scale independence in terms of the extent to which development fills the space available. The model adopted here can be stated as

$$p(R) = KR^{-\alpha}, \quad (5)$$

where α is a parameter related to the spread of the function, and K is a normalizing constant.

It is thus possible to show, given limits on the range of equation (5), that the cumulative population $N(R)$ associated with the density $p(R)$ can be modeled as

$$N(R) = GR^{2-\alpha}, \quad (6)$$

where G is some constant. From equation (6) it is clear that the area $A(R)$ over which density is defined with respect to distance from the CBD is given by

$$A(R) = ZR^2, \quad (7)$$

where Z is some constant. For an area which is enclosed by a perfect circle, $Z = \pi$. There are very strong connections between urban density and urban allometry based on equations (5)–(7), but the most appealing link between these relations is through ideas from fractal geometry which seek, through the concept of fractal dimension, to relate density to the extent to which population fills space. The rationale for these links has been developed extensively (Batty and Longley, 1994; Frankhauser, 1994; Longley et al, 1991), and in this paper we will only document results. In short, the power law defined by equation (6) is consistent with systems whose activities are distributed according to the principle of similitude or self-similarity. Such laws thus apply whatever the scale. In this context, it is easy to show that the density parameter α is related to the fractal dimension, D , that is,

$$D = 2 - \alpha,$$

and that the cumulative population relation can be written as

$$N(R) = GR^D, \quad (8)$$

where D is a measure of both the extent and the rate at which space is filled by population with increasing distance from the CBD.

Fractal geometry provides a much deeper insight into density functions than has been available hitherto, in that it provides ways in which the form of development can be linked to its spread and extent. In this paper we do not discuss form per se but simply concentrate upon the values of the parameters as measures of the way spaced is filled and the rate at which this space-filling changes with respect to distance from the CBD. In fact, the parameters D and α both measure more than one effect. First, as these parameters are related to the slopes of their respective functions, they can be used to detect the attenuation effects of distance. At the same time, the extent to which space is actually filled is also measured by D and α .

This interpretation is both important and problematic. It is argued that in urban systems the fractal dimension of any development should lie between 1 and 2; that

cities (and their land uses) fill more than the linear extent of the two-dimensional space in which they exist (where $D = 1$) but less than the entire space ($D = 2$). Notwithstanding the notion that cities may fill some of their 'third dimension', the way we define density as simple occupancy of space means that we constrain the dimension to lie between 1 and 2. However, D and α also measure the attenuation effects, and it is quite possible for these parameters to take on values outside the range 1-2 if significant changes in the slopes of their respective functions occur over the distances used to detect them. Accordingly, we have developed several techniques for estimating dimension, the first set of which emphasizes space-filling, the second set, density attenuation.

4 Estimating fractal dimensions

The simplest method, and perhaps the most robust, involves approximating the dimension from the models of occupancy based on various forms of idealized lattice. Consider a square lattice centrally positioned on the CBD, each square of the grid being either occupied (developed) or not. Then, if every square were occupied (with the implication that $D = 2$), then the sequence of occupancy would be as follows: first, for 1 unit of spacing (or distance), 4 points would be occupied; for 2 units, 16 points occupied; for 3 units, 36 points occupied; and so on. In this case, it is clear that the relation is given by $N(R) = 4R^2 = (2R)^2$, and therefore we might approximate this for a grid which is less than entirely occupied as $N(R) = 4R^D$. Thus, for any value of R , we can compute directly the value of D or α . As we argue below, probably the most appropriate value for R is the mean distance, R' , which, for a discrete distribution of populations n_i where i indicates the grid location, is given as

$$R' = \frac{\sum_i n_i R_i}{\sum_i n_i},$$

Note that R_i is the distance from the core to i . Using R' , we calculate the dimension as follows,

$$D = \frac{1}{\log_{10} R'} \log_{10} \left[\frac{N(R')}{4} \right]. \quad (9)$$

This is our first estimate of dimension from which α can be computed as $2 - D$.

Equation (9) depends upon the constant being known, and strictly this constant is not 4 but 2^D or, in the case of a continuous system, π . However a simple translation of this involving density rather than cumulative population removes this restriction. The area $A(R)$ of the grid is proportional to its full occupation, that is, $A(R) = ZR^2$. Forming the density directly from equations (7) and (8) gives

$$\begin{aligned} p(R) &= \frac{GR^D}{ZR^2} \\ &\approx R^{D-2} = R^{-\alpha}, \end{aligned} \quad (10)$$

where we assume that $G \approx Z$. Rearranging equation (10) gives a second estimate of dimension for any value of R . Thus, for the mean value R' , D is given by

$$D \approx 2 + \frac{\log_{10} p(R')}{\log_{10} R'}. \quad (11)$$

Clearly, the dimensions in equations (9) and (11) can be computed by using values of R other than the mean R' , but we restrict our usage to the mean here, which has been found in previous work to give the best estimates (Batty and Longley, 1994). Last, from these equations, it is clear that D must lie between 1 and 2.

The two methods of estimation defined so far do not take account of any variance within the distributions other than through the use of the mean. However, an obvious and well-used method is to linearize the power laws for density as in equation (5) and/or for the cumulative population relation in equation (6) and perform regression to give values for K and α and/or for G and D , respectively. These linearized forms are given as follows for the case where discrete densities p_i and cumulative populations N_i are defined. Then,

$$p_i = \log_{10} K - \alpha \log_{10} R_i, \quad (12)$$

$$N_i = \log_{10} G - D \log_{10} R_i. \quad (13)$$

From these equations, we can compute the whole range of performance measures associated with linear regression, and we will use the square of the correlation coefficient, r^2 , as a measure of fit. This will give us some idea of the strength of the relationships. Also, because equations (12) and (13) are related to one another, the parameter values of α and $2 - D$ will be identical for consistently defined data (see Batty and Kim, 1992).

The regression method of estimation can generate fractal dimensions which are outside the logical limits associated with space-filling in two dimensions. Because the slope parameters in equations (12) and (13) measure the rate at which density attenuates and population increases with respect to distance, dimensions greater than 2 occur when physical constraints restrict development near the CBD or when density profiles show major departures from the norm of monotonic decline from the core. Values less than 1 can also occur if reversals from the norm appear. In both of these cases, the divergence of dimension outside the range $1 < D < 2$ is reflected in the value of the intercept constants K and G in equations (12) and (13). However, if these constants are constrained to values which reflect idealized space-filling, then estimates of α and D will be within the space-filling limits. In this way, a measure of the variance in the distribution of densities and populations can be accounted for through constrained regression. This is tantamount to replacing the constant K in equation (12) with a value such as 1, and G in equation (13) with a value such as 4 or π . We will use these constraints in the empirical work which follows.

5 Constructing the land-use surfaces

The two images used to create the surfaces reflecting early-1980s and late-1980s distributions of urban land use in Bristol are based upon the Landsat TM-5 three-band (blue, red, green) image taken on 26 April 1984, and the SPOT HRV, three-band, false-color, 1024×1024 pixel satellite images taken on 18 June 1988. These images were judged to be sufficiently different to measure land-use change which we grounded in socioeconomic data taken from the 1981 and 1991 Population Censuses. Hereafter, we refer to these as 1981 and 1991 distributions, although the usual caveats apply where data are being synthesized from sets at different points in time. The methods outlined in section 2 and illustrated in figure 1 were applied. This procedure involves taking each image and identifying relevant land-use categories which are taken from census variables by using the training samples explained earlier. In figure 2 we show the two elements of this process—the 1984 Landsat and 1988 SPOT HRV images (in terms of the urban-rural contrast in the blue

wavelength), and examples of the 1981 and 1991 numbers of household surfaces (in terms of a threefold gray-scale classification) which are used in the process of creating the residential-housing land-use category. Also shown is a schematic map of the study area, urban Bristol, illustrating the main route network and physical constraints on the development, to provide the reader with some sense of the scale of the problem.

After each surface was generated with respect to each land-use category, each scene was processed by means of the Unix-based ERDAS software, geo-referenced

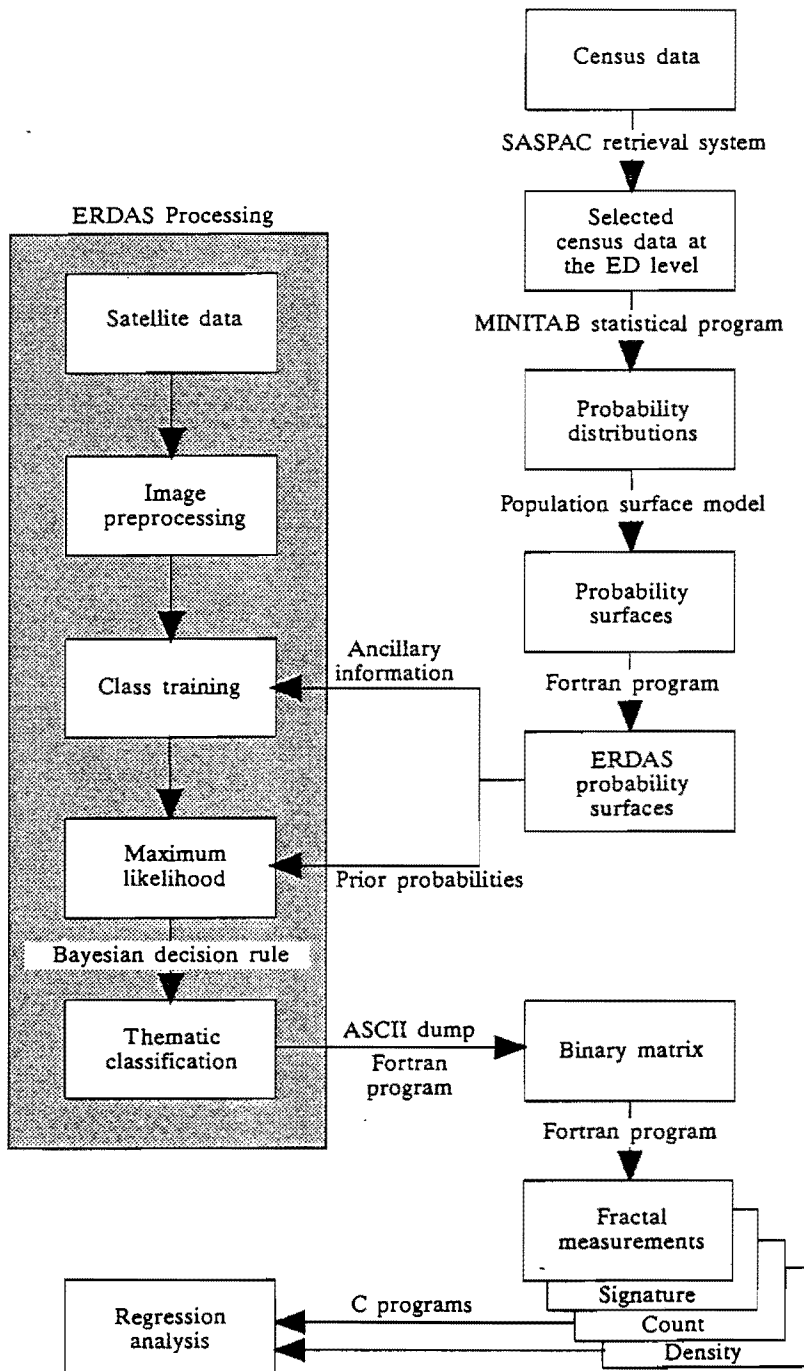
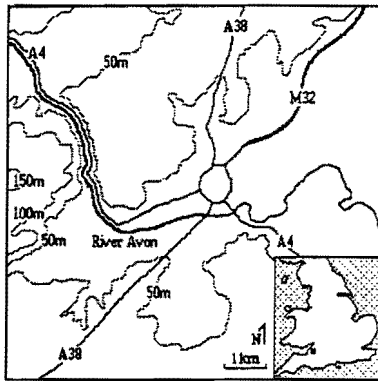
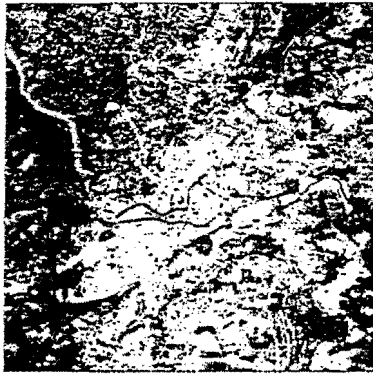


Figure 1. The procedure for generating land-use categories from the remotely sensed data. Note: ED, enumeration district.

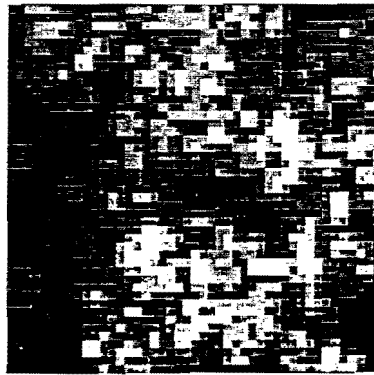
by ground control points with a first-order bilinear interpolation and classified by using the specially modified maximum likelihood algorithm sketched above in section 2. Nonurban areas were first excluded with a standard spectral density slice as indicated by figure 2. For the 1981/1984 data, four land-use categories were defined: first, urban land as defined by the Office of Population Censuses and Surveys (Longley et al, 1992); second, built-up land, a more restrictive definition than the first but both of these categories being defined by use of spectral values only; third, residential land; and, fourth, nonresidential land, both defined with respect to the population count and household size surfaces. These were the only relevant variables in the 1981 Census which were consistent with the 1991 Census.



The Bristol urban area



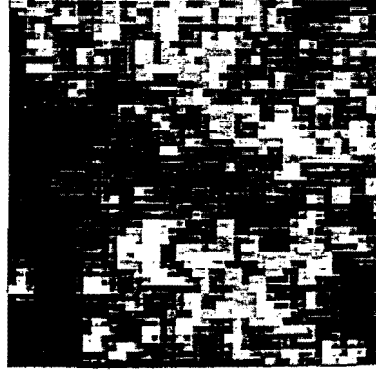
Landsat TM-5 image, 26 April 1984



Residential-housing surface, 1981



SPOT HRV image, 18 June 1988



Residential-housing surface, 1991

Figure 2. The basic data: the 1984 and 1988 images of Bristol and the 1981 and 1991 residential surfaces.

For the 1988/1991 data, these first four categories were also defined under identical criteria, but four others were added because of the availability of census data. These were: fifth, detached housing; sixth, semidetached housing; seventh, terraced housing; and, eighth, residential flats. Each of these last four categories is based on the numbers of detached, semidetached, terraced, and flatted properties in each 100 m grid square of the associated surfaces. The final land-use categories for each of the two years were then compiled simply by selecting the maximum probability for each pixel in the image. Thus, for each year in question,

$$L_{ik} = \begin{cases} 1, & \text{in land-use category } k, \text{ if } P_{ik} = \max_w P_{iw}, \\ 0, & \text{otherwise.} \end{cases} \quad (14)$$

The four surfaces for 1981 are shown in figure 3 (see over), the eight for 1991 in figure 4. These form the basic data upon which the empirical analysis is accomplished.

The density analysis first requires the definition of a central 'seed' site about which the urban area is deemed to have grown, and in the Bristol case we have taken the historical center to be the Bristol Bridge. The 1988/1991 SPOT HRV image was then reduced to a 453×453 pixel subsection centered upon the bridge, and, as the nominal spatial resolution is 20 m, the geographic coverage is $9060 \text{ m} \times 9060 \text{ m}$ ($82\,084 \text{ km}^2$). The 1981/1984 Landsat image has a resolution of 30 m, and this was then sectioned and scaled to the same area. These requirements are necessary for all subsequent analyses of urban density measurements in this paper. To organize the data for this analysis, we then counted the numbers of cells of each land use in successive rings of about 13 m width, thus giving the variables we refer to subsequently as the 'count' values N_i (where i now refers to the individual ring). These counts, when normalized by area of each ring, form the densities p_i , and each of these densities is defined for the land uses in question. The cumulative count and density profiles are based on these definitions. We are now, at last, in a position to present the empirical analysis.

6 Applications to land-use densities in Bristol

The first measures of density and dimension are close to the idea of measuring the occupancy of each land use, and give values between 1 and 2, that is, fractal dimensions which show that each land use fills more than a line across the space ($D = 1$) but less than the complete plane ($D = 2$). Equations (9) and (11) were applied to the surfaces in figures 3 and 4, yielding the dimensions shown in table 1. There is remarkable consistency in these estimates between land uses at each time slice. First, all the estimates fall in the range $1.399 < D < 1.837$, with the mean

Table 1. Space-filling dimensions, based on occupancy class.

Land-use category	Equation (9) of text		Equation (11) of text	
	1981	1991	1981	1991
Urban	1.780	1.817	1.795	1.837
Built-up	1.776	1.808	1.790	1.826
Residential	1.756	1.777	1.768	1.792
Nonresidential	1.598	1.568	1.598	1.556
Detached housing		1.556		1.542
Semidetached housing		1.604		1.596
Terraced housing		1.663		1.630
Apartments or flats		1.399		1.362

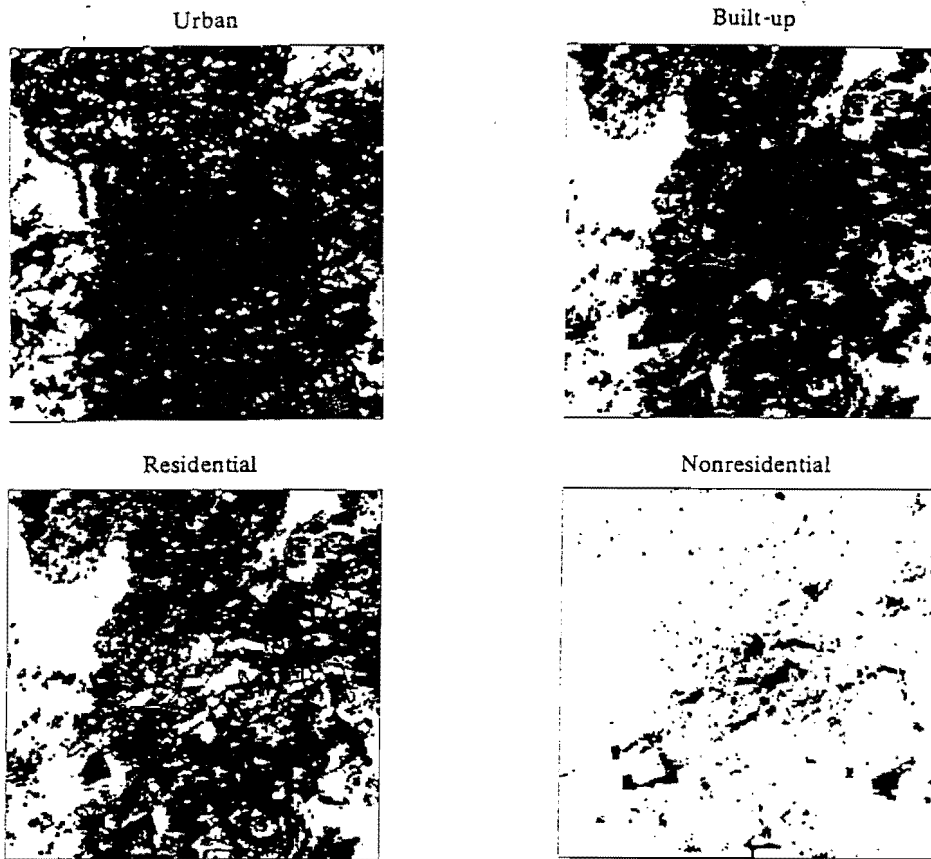


Figure 3. The 1981 binary land-use surfaces.

value of D over all land uses, the two time points, and the two equations being 1.673. The theory of the fractal city sketched out elsewhere by two of the authors (Batty and Longley, 1994) argues that cities are likely to have fractal dimensions between 1.66 and 1.71, which are those consistent with randomly constrained diffusion processes such as DLA (diffusion-limited aggregation) (Vicsek, 1989). The results bear out these notions.

The order given by the fractal dimensions [$D(\text{land use})$] with respect to all land uses is also consistent between the estimates from the two equations and from the two time slices. This order is

$$D(\text{urban}) > D(\text{built-up}) > D(\text{residential}) > D(\text{terraced}) > D(\text{semidetached}) \\ > D(\text{nonresidential}) > D(\text{detached}) > D(\text{apartments or flats}),$$

and there are no reversals of rank in any of the four columns of table 1. There is perhaps a logic to the absolute values of these dimensions too. Urban, built-up, and residential land uses clearly occupy more space than any of their disaggregates, and the order within these three land uses also reflects that 'residential' is a proper subset of 'built-up', which in turn is a proper subset of 'urban'. In terms of property types, 'terraced' and 'semidetached' are likely to be most clustered in the city than 'detached' and 'apartments or flats', and the values generated are similarly consistent. 'Nonresidential' is a residual category, the complement of the residential land-use set, and as such there is an obvious relation between each. However, although it may be possible to derive one fractal dimension from the other, it is not clear how this might be done in terms of equations (9) or (11) because of the

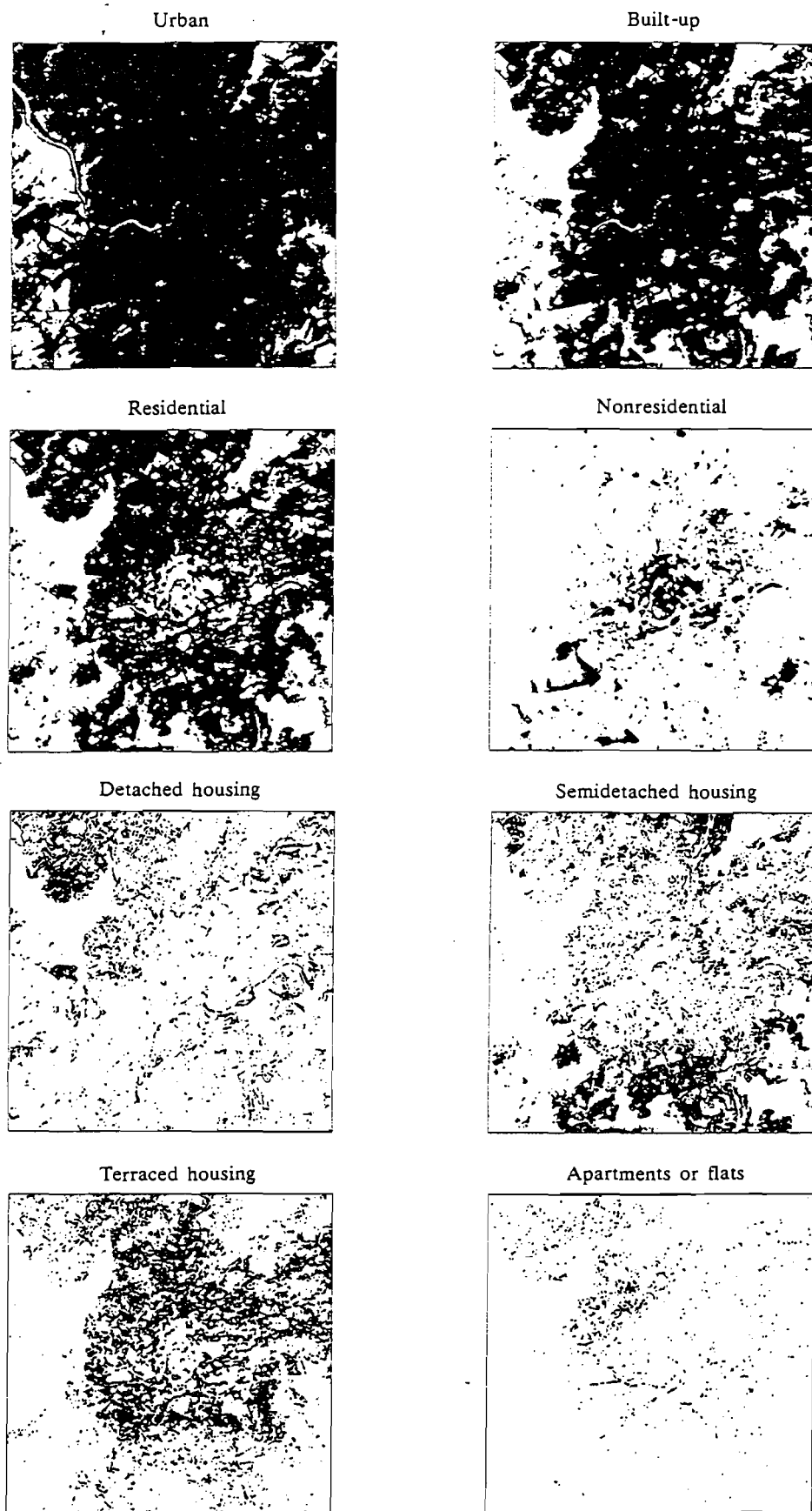


Figure 4. The 1991 binary land-use surfaces.

definition of the mean distances R' . This is a matter for further research. The last substantive point relates to the change in dimensions between the 1981/1984 and the 1988/1991 data. There is a small but significant increase in the dimensions of urban, built-up, and residential land use over this period, with a slight decrease in that for nonresidential land use. This is consistent with urban growth in this period but to generate stronger conclusions, more and better temporal information is required.

The two types of estimate just presented do not account for the variance in each land-use pattern and thus it is impossible to speculate upon the shapes of these patterns with respect to density profiles. Thus the main body of analysis is based on fitting regression lines to the profiles generated from each surface in terms of the count of land-use cells in each circular band from the core (the Bristol Bridge), given as N_i , and their normalization to densities, p_i . These data are then used to estimate the parameters in equations (8) and (5), respectively, from their logarithmic transforms in equations (13) and (12), respectively. The profiles based on the count and density for the four land-use categories in 1981 are shown in figures 5 and 6, and the same profiles for the eight categories for 1991 are shown in figures 7 and 8 (see over).

Some comment on these profiles is required. There are strong similarities between the 1981 and 1991 graphs for the same land uses, as might be expected from data which are, in part, only four years different in terms of the remotely sensed images, and this also provides some check on the confidence we have in our methods for extracting land uses. But the most significant features pertain to the density plots, which reveal the existence of clear physical constraints on development in our example (see figures 6 and 8). These densities fall in the manner anticipated as distance increases away from the core for all land uses in both of the time periods. For the disaggregate housing land uses this decline is steepest, but at

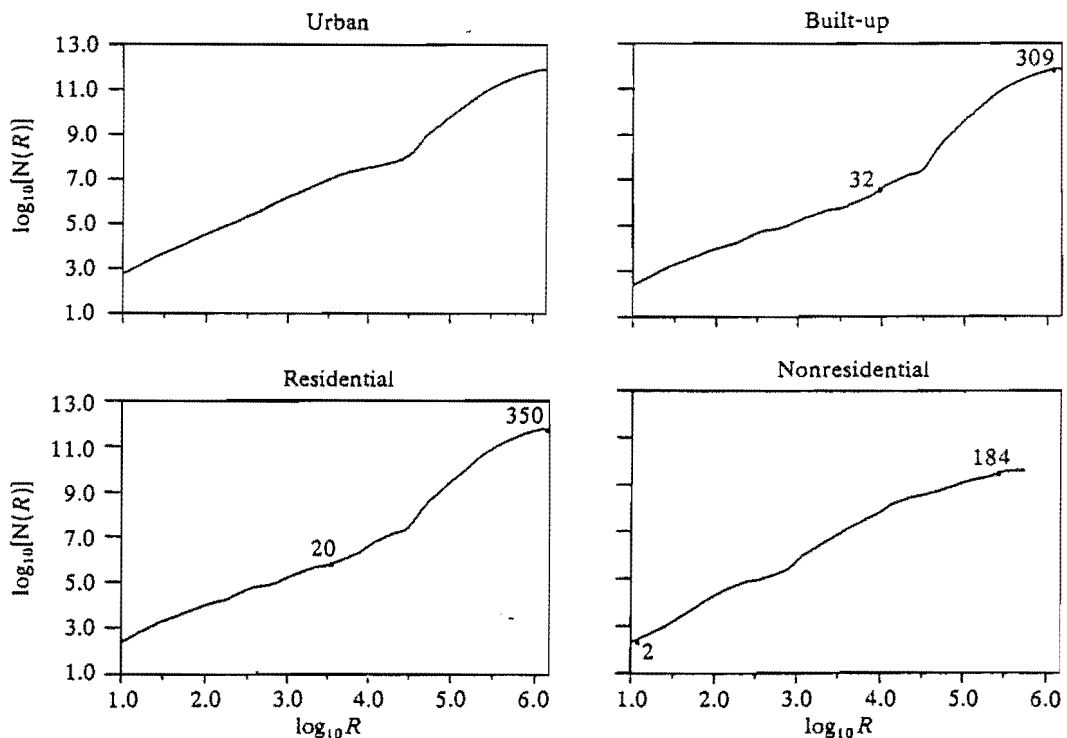


Figure 5. The 1981 count profiles for four land uses defined. Note: numbers within the graphs are the zone numbers of the data points indicated.

a distance of about 3–4 km from the core, the city is cut by river valleys and gorges (see figure 2). Once these, and other (for example, public open space) constraints are passed, land uses increase in density quite rapidly, soon peaking, then declining again in the manner expected. This is bound to lead to poor estimates of performance in terms of fitting these profiles by means of equation (12). For the cumulative counts shown in figures 5 and 7, these reversals simply manifest themselves in terms of breaks in slope, but the implications of fitting equation (13) to these graphs is that fractal dimensions are likely to exceed 2 in several cases.

The results of fitting equations (12) and (13) to all land uses from each of the time slices are shown in table 2. The parameter estimates from each of these equations are identical, but the performance measures based on r^2 differ substantially. For the fractal dimensions, the order is quite different from that associated with the occupancy values in table 1. There is little point in commenting on the order, although it is consistent for both time slices, as this order reflects the gradient changes arising from physical constraints. In fact, only for detached housing and flats is a clear inverse distance decay of densities observed, and this is reflected in the fact that the fractal dimensions of these profiles are in the correct range and give high r^2 values both for counts and for densities. The performance of the count distributions is good, as is always the case with cumulative profiles.

Examination of the profiles in figures 5–8 reveals immediately the problems which are reflected in table 2. There are two ways in which we might generate more 'acceptable' dimensions from these data. First, we can constrain the regression by fixing the intercept values in advance, for, as we indicated above, this will ensure that the values fall within the range $1 < D < 2$ (subject to a normal error range). Second, we can reduce the range of the plots over which these regressions are made, thus cutting off extreme segments and omitting outliers. We will develop the

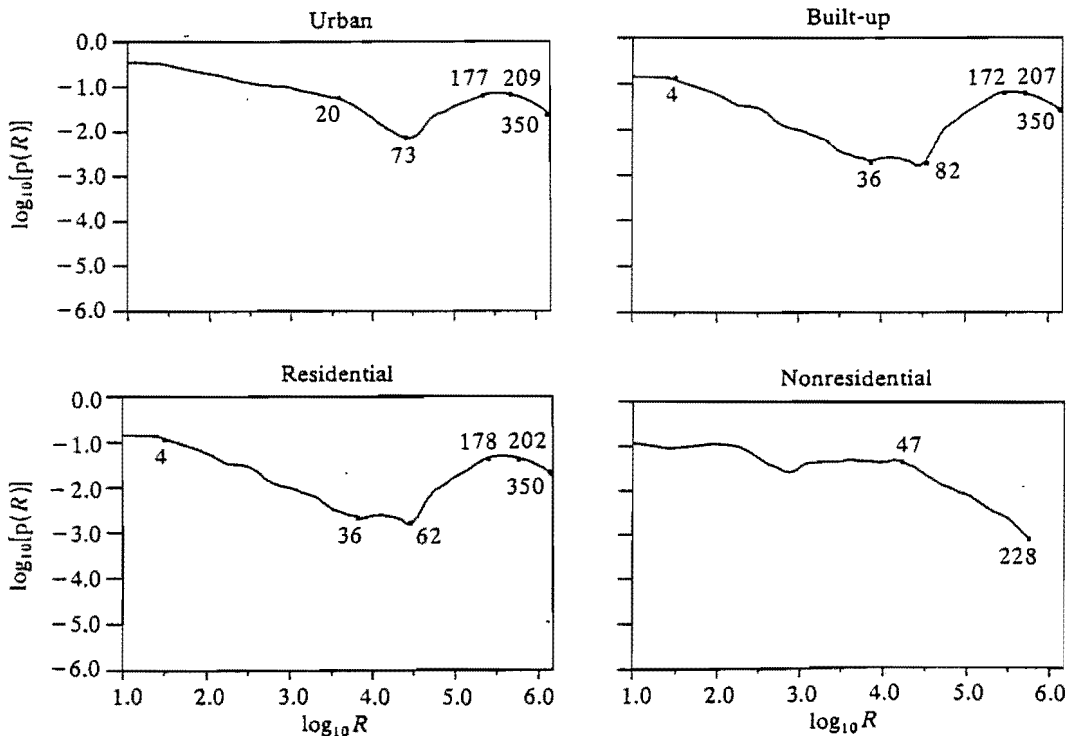


Figure 6. The 1981 density profiles for the four land uses defined. Note: see figure 5.

constrained regression first, and the results of fitting equations (12) and (13) in this way are presented in table 3. With this method, the fractal dimensions generated for the count and the densities now differ. In general, the performance of the estimates improves for the density profiles and worsens slightly for the counts, but these results are not significant. What does happen as expected is that all the values generated fall now within the range $1 < D < 2$, with the exception of the urban density profile for 1991, which yields a D value of 2.012 from equation (13).

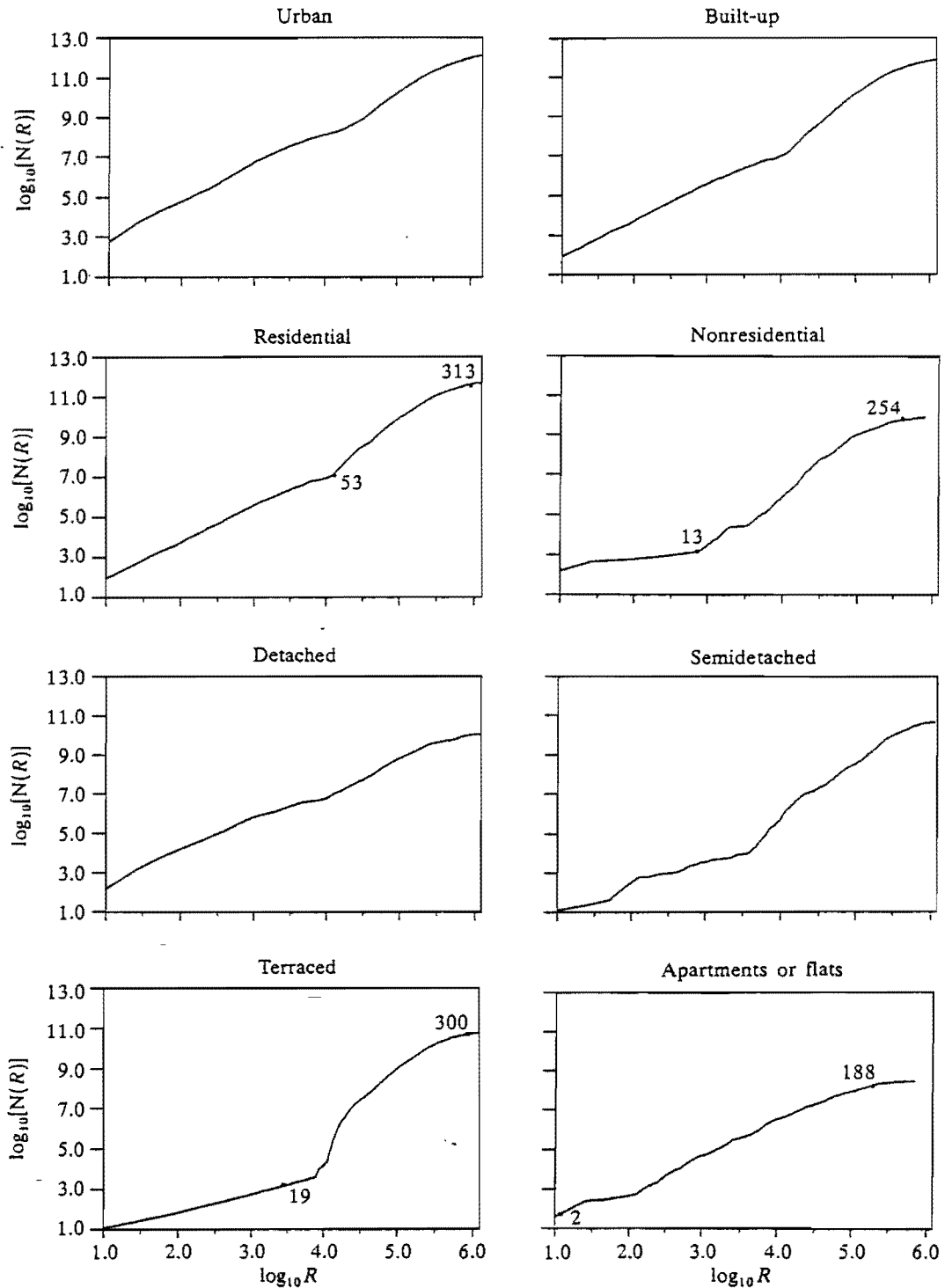


Figure 7. The 1991 count profiles for the eight land uses defined. Note: see figure 5.

This is because the fact that the intercept values which have to be fixed in advance are always approximations to an unknown value which will ensure the constraints are met. In fact, it is likely that the intercept values used should be higher, and thus this would lower the dimensions a little in all cases, enough to keep all values within the range.

The order of values generated in this way now corresponds much more closely to that noted above for dimensions associated with equations (9) and (11).

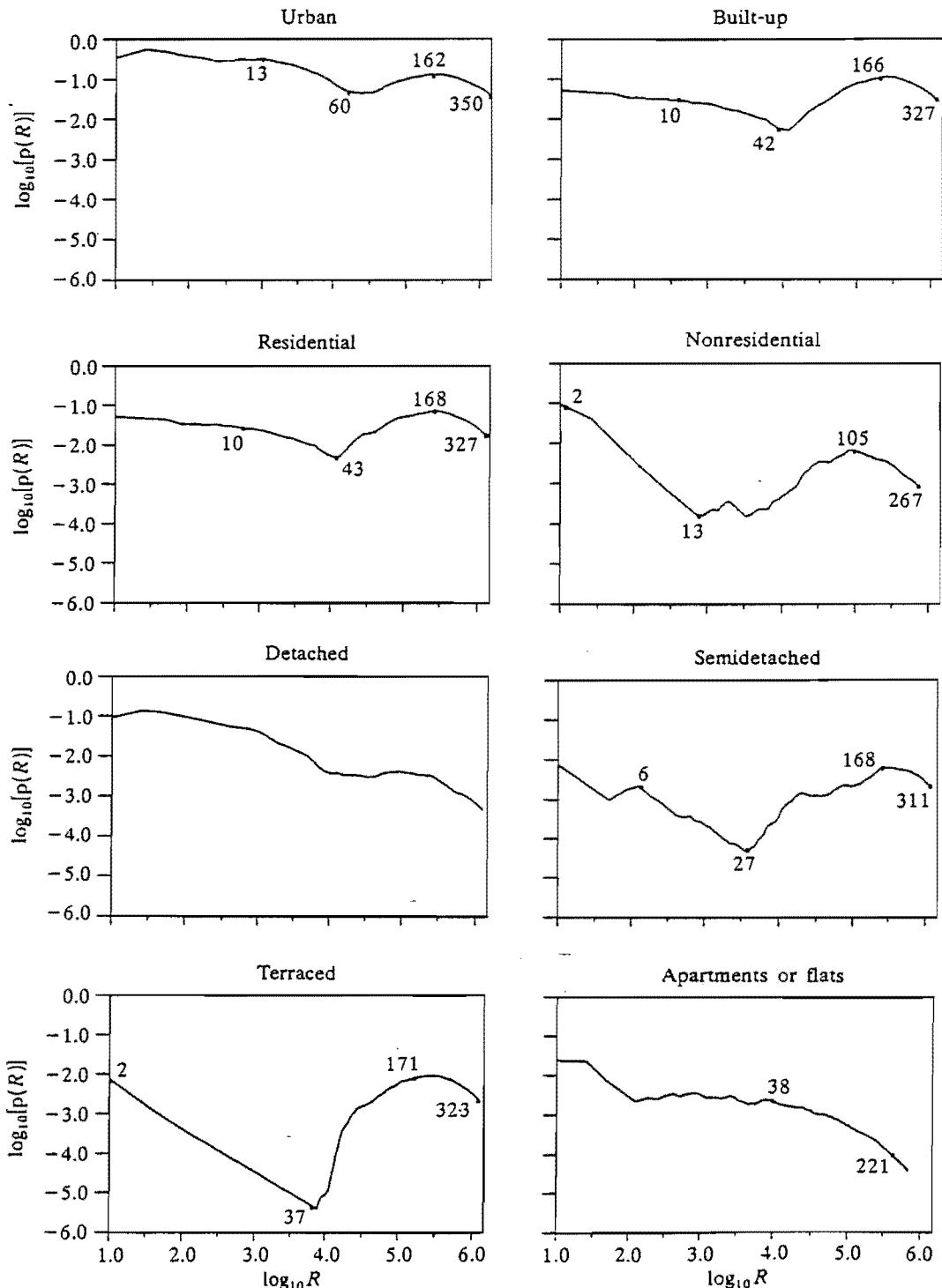


Figure 8. The 1991 density profiles for the eight land uses defined. Note: see figure 5.

Table 2. Dimensions, D , from regression of equations (12) and (13) in text, and r^2 values for equations (12) and (13) ($r_{(12)}^2$ and $r_{(13)}^2$, respectively).

Land-use category	1981 data			1991 data		
	D	$r_{(12)}^2$	$r_{(13)}^2$	D	$r_{(12)}^2$	$r_{(13)}^2$
Urban	1.988	0.002	0.977	1.861	0.335	0.989
Built-up	2.293	0.304	0.964	2.190	0.274	0.980
Residential	2.251	0.264	0.966	2.123	0.179	0.983
Nonresidential	1.429	0.802	0.962	2.118	0.060	0.953
Detached housing				1.534	0.873	0.986
Semidetached housing				2.375	0.529	0.978
Terraced housing				2.657	0.490	0.940
Apartments or flats				1.407	0.824	0.964

Table 3. Dimensions, D , obtained from the constrained regression, and r^2 values. Note: subscripts (12) and (13) indicate the data applying to equation (12) and equation (13), respectively.

Land-use category	1981 data				1991 data			
	$D_{(12)}$	$r_{(12)}^2$	$D_{(13)}$	$r_{(13)}^2$	$D_{(12)}$	$r_{(12)}^2$	$D_{(13)}$	$r_{(13)}^2$
Urban	1.741	0.033	1.954	0.960	1.800	0.483	2.012	0.935
Built-up	1.709	0.302	1.921	0.808	1.759	0.347	1.973	0.883
Residential	1.691	0.325	1.903	0.917	1.730	0.374	1.944	0.898
Nonresidential	1.557	0.622	1.787	0.831	1.479	0.267	1.701	0.766
Detached housing					1.498	0.941	1.713	0.908
Semidetached housing					1.510	0.691	1.727	0.711
Terraced housing					1.523	0.356	1.738	0.615
Apartments or flats					1.313	0.954	1.539	0.949

The order for the 1991 data for both the count and density land-use categories in terms of D is

$$D(\text{urban}) > D(\text{built-up}) > D(\text{residential}) > D(\text{terraced}) > D(\text{semidetached}) \\ > D(\text{detached}) > D(\text{nonresidential}) > D(\text{apartments or flats}),$$

and this is the same as that noted above, with the exception of $D(\text{nonresidential})$, which moves down a couple of ranks. The 1981 data are consistent with this order too, with the values increasing a little for urban, built-up, and residential land uses for both count and density over the time period, with the value for nonresidential land uses falling a little. One interesting difference is that the estimates of dimensions from the density profiles are higher by around 0.2 in value than those from the count, but this is likely to be a result of the different intercept values used. One issue has become very clear from this analysis and this is that space-filling and the attenuation of densities are different aspects of morphology and that, in future work, some attention should be given to the extent to which different dimensions can be developed to reflect this.

The second method of refining the dimensions involves cutting down the set of observations which constitute the population density and count profiles. In terms of a theory of the fractal city, if such cities are generated according to some diffusion about a seed or core site, as historic cities in the industrial and preindustrial ages clearly were, then it is likely that the profiles observed show departures from inverse distance relations in the vicinity of the core and the periphery. Around the core, population has been displaced, whereas on the periphery the city is still

growing, and thus the inverse relation will be distorted. It is standard practice to exclude observations in these areas, and, in previous work (Batty et al, 1989), dimensions have been refined by using such exclusions. In the case of the Bristol profiles, this issue is further complicated by the existence of the physical constraints on development because of the river gorges which cut through the city. Accordingly, we have taken the profiles in figures 5-8 and simply fitted the density and count relations to their various linear segments.

The count profiles for 1981 and 1991 shown in figures 5 and 7 have characteristic profiles for all land use involving a single break in slope: most uses accumulate slowly up to the gorge areas of the city and then increase suddenly, thus producing fractal dimensions greater than those generated by the simpler occupancy equations (9) and (11). For some land uses, particularly nonresidential land use, this pattern is reversed, in that the break in slope is from steep to less steep, when the gorges are encountered. In table 4, we have selected three count profiles for 1981 and four for 1991 and have performed the regressions implied by equation (13) for restricted portions of the curves indicated in figures 5 and 7 and noted in terms of zones. Most of these regressions emphasize the steepest parts of these curves and yield dimensions greater than 2, thus illustrating the effect of physical constraints on the development of the city. Constrained regressions are less meaningful in this context, although these can still be considered relevant for the portion of the curves considered. However, these have been excluded.

Table 4. Dimensions, $D_{(13)}$, associated with partial population counts, based on equation (13) in text, and associated $r_{(13)}^2$ values.

Land-use category	1981 data			1991 data		
	zone range ^a	$D_{(13)}$	$r_{(13)}^2$	zone range ^a	$D_{(13)}$	$r_{(13)}^2$
Built-up	32-309	2.774	0.978			
Residential	20-350	2.536	0.977	53-313	2.093	0.968
Nonresidential	2-184	1.518	0.973	13-254	2.310	0.955
Terraced housing				19-300	3.034	0.942
Apartments or flats				2-188	1.545	0.985

^a This shows the zone numbers which are included in the regressions, where there are 350 zones in the complete set. The ranges implied by these numbers are shown in figures 5 and 7.

Reducing the range of density profiles, however, is likely to provide more significant results, for the profiles are distorted in characteristic manner over all land uses. For both 1981 and 1991, as figures 6 and 8 reveal, the curves decline in the usual manner but at a faster rate than might be anticipated in the absence of constraints. Hence, once the gorge areas have been crossed, densities increase and then decline again following the more usual pattern. The obvious partition is thus into three linear segments, each of which can be fitted by equation (12). We have not divided all four land uses in 1981 and all eight in 1991 into these three segments but we have concentrated upon those curves where breaks in slope are most significant.

These breaks are indicated on the profiles in figures 6 and 8, and the associated dimensions and r^2 values are presented in table 5 (see over). For both 1981 and 1991 the two segments of these profiles which decline inversely with distance yield dimensions much lower than expected, that is, nearer 1 than 1.7, whereas the positive segments of these curves give dimensions greater than 2. The model fits, however, are good, with r^2 values all greater than 0.8 and most over 0.95. Yet all this analysis

on urban development, it becomes exceptionally difficult to unravel the effect of distortions at the core and the periphery which still need to be excluded if the equilibrium fractal dimensions are to be measured. This clearly requires further research as we begin to augment our research to embrace more thoroughly than any previous research the role of constraints on fractal dimension and density.

Table 5. Dimensions, $D_{(12)}$, associated with partial population densities based on equation (12) in text, and associated $r_{(12)}^2$ values.

Land-use category	1981 data			1991 data		
	zone range ^a	$D_{(12)}$	$r_{(12)}^2$	zone range ^a	$D_{(12)}$	$r_{(12)}^2$
Urban	20-72	1.083	0.955	13-60	1.309	0.960
Urban	73-177	2.816	0.964	162-350	1.234	0.952
Urban	209-350	1.065	0.964			
Built-up	4-36	1.203	0.993	10-42	1.446	0.949
Built-up	62-172	3.531	0.950	166-327	1.076	0.959
Built-up	207-350	1.134	0.951			
Residential	4-36	1.203	0.993	10-43	1.431	0.946
Residential	62-178	3.366	0.955	168-327	1.105	0.958
Residential	202-350	1.186	0.940			
Nonresidential	47-228	0.927	0.990	2-13	0.452	0.996
Nonresidential				105-267	0.995	0.961
Semidetached				6-26	0.914	0.987
Semidetached				27-167	2.826	0.880
Semidetached				168-311	1.326	0.865
Terraced housing				2-36	0.898	0.999
Terraced housing				37-170	3.617	0.802
Terraced housing				171-323	1.012	0.954
Apartments or flats				38-221	1.113	0.950

^aThis shows the zone numbers which are included in the regressions, where there are 350 zones in the complete set. The ranges implied by these numbers are shown in figures 6 and 8.

7 Conclusions: future research

The theory of the fractal city requires extensive empirical testing through the development of typologies based on different urban morphologies. Using the concept of fractal dimension and its relation to density, we have made a start upon this quest, but its successful embodiment depends upon the existence of widely available data to define urban form, data which enable consistent comparisons between case studies. Remotely sensed data fulfill this role. The methods developed here can be applied routinely, thus generating consistent land-use classifications for different examples, and the existence of a universal data set which is continually being updated enables many different types of city forms to be explored through time. There is no other data set which has such properties of generality, and although comprehensive digital data exist in the USA (for example, from the TIGER files) this is manually collected in the first instance and cannot be used for the kind of temporal analysis essential to questions of urban growth. There are problems in classifying such images into land-use categories, but there is much research on this frontier at present within remote sensing, which bodes well for better classifications. There are even possibilities for improving image analysis by means of fractal statistics, which are naturally occurring measures for such images (de Cola, 1993).

In this paper, we have been able to extend our analysis to different land uses and to begin some rudimentary analysis of their change over time in terms of their morphology. A widely recognized focus within contemporary urban theory

concerns the evolution of cities, and, in this regard, we see remotely sensed imagery as the database upon which we can truly develop the dynamics of the city in fractal terms (Dendrinis, 1992; Longley and Batty, 1993). For changes in fractal dimension through time, fractal theory is well worked out in terms of growth dynamics (Vicsek, 1989) but there is much more work to be done on how the morphologies of individual land uses coalesce to produce more aggregate morphologies of urban development.

Here we have produced fractal dimensions for urban development and then for the land uses which compose it. As yet, we have no formal theory as to how the fractal dimensions of individual land uses 'add up' to those of the whole. For example, the four housing types defined from the 1991 data form when aggregated the residential class. The question is 'how do the individual dimensions $D(\text{land use})$, where land use = terraced, semidetached, detached, and apartments or flats, combine to produce $D(\text{residential})$?' There is some formal theory to be developed here which involves an extension of fractal theory per se and thus might be applicable to any problem of a form in which the parts add up to the whole. This is a question we intend to address in future work.

Finally, the example of Bristol we have chosen is one which illustrates how problematic the analysis becomes when several physical constraints distort the development of the city. So far, in our more general research program concerning the analysis of urban form by use of fractals, we have concentrated upon cities which have been developed in relatively unconstrained situations, or we have dealt with cities where physical constraints have been well defined because of natural features such as rivers and estuaries which rule out development completely (Batty and Longley, 1994). The Bristol example we have dealt with here extends our approach considerably, thus raising two issues. First, new measures are required which distinguish between the space-filling function of the fractal dimension and its reflection of the attenuation of densities. This suggests that D might be used purely for space-filling as implied by equations (9) and (11), and that a new measure of the effect of attenuation be composed from $D (= 2 - \alpha)$ and K in equation (12), say. Calling D in equation (12) D^* , then we might construct indices which measure the combined effect of D^* and K relative to some idealized space-filling norm, or we might take differences between D and D^* . All of these are for the future, but work in this area has implications for fractal theory beyond the immediate domain of urban systems. The development of constrained regression might be improved too. The selection of predetermined constants is problematic; the lattice-based example which we have treated here as the ideal type is in itself an approximation, and more thought is needed concerning this.

Nevertheless, what we have shown in this paper is that morphology can be extracted from remotely sensed data and be measured by calling upon new ideas which link fractal theory with urban density. The ultimate quest in this work is, of course, the development of a classification of morphologies based on a deeper understanding of how urban processes lead to cities of different shapes and densities. There are many policy implications stemming from such work, particularly involving accessibility and energy use as well as questions of social and economic segregation. It is our view that we are at the beginning of developing useful ideas in this domain. The existence of remotely sensed imagery and its classification in terms of urban land use, as we have developed here, will speed progress towards the goal of understanding how cities fill the space available to them and of how distortions to this process through policy intervention might affect issues of spatial efficiency and equity.

References

- Arlinghaus S L, 1985, "Fractals take a central place" *Geografiska Annaler B* 67 83-88
- Arlinghaus S L, 1993, "Central place fractals: theoretical geography in an urban setting", in *Fractals in Geography* Eds N S-N Lam, L de Cola (Prentice-Hall, Englewood Cliffs, NJ) pp 213-227
- Batty M, Kim K S, 1992, "Form follows function: reformulating urban population density functions" *Urban Studies* 29 1043-1070
- Batty M, Longley P A, 1994 *Fractal Cities: A Geometry of Form and Function* (Academic Press, London)
- Batty M, Longley P A, Fotheringham S, 1989, "Urban growth and form: scaling, fractal geometry, and diffusion-limited aggregation" *Environment and Planning A* 21 1447-1472
- Bracken I, Martin D J, 1989, "The generation of spatial population distributions from census centroid data" *Environment and Planning A* 21 537-543
- Clark C, 1951, "Urban population densities" *Journal of the Royal Statistical Society (Series A)* 114 490-496
- de Cola L, 1993, "Multifractals in image processing and process imagining", in *Fractals in Geography* Eds N S-N Lam, L de Cola (Prentice-Hall, Englewood Cliffs, NJ) pp 213-227
- Dendros D S, 1992 *The Evolution of Cities* (Routledge, London)
- Frankhauser P, 1994 *La Fractalité des Structures Urbaines* (Anthropos, Paris)
- Langford M, Maguire D J, Unwin D J, 1991, "The areal interpolation problem in estimating population using remote sensing in a GIS framework", in *Handling Geographical Information* Eds I Masser, M Blakemore (Longman, Harlow, Essex) pp 55-77
- Longley P, Batty M, 1989a, "Fractal measurement and cartographic line generalisation" *Computers and Geosciences* 15 167-183
- Longley P, Batty M, 1989b, "On the fractal measurement of geographical boundaries" *Geographical Analysis* 21 47-67
- Longley P A, Batty M, 1993, "Speculation on fractal geometry in spatial dynamics", in *Nonlinear Evolution of Spatial Economic Systems* Eds P Nijkamp, A Reggiani (Springer, Berlin) pp 203-222
- Longley P, Batty M, Shepherd J, 1991, "The size, shape and dimension of urban settlements" *Transactions of the Institute of British Geographers: New Series* 16 75-94
- Longley P A, Batty M, Shepherd J, Sadler G, 1992, "Do green belts change the shape of urban areas? A preliminary analysis of the settlement geography of South East England" *Regional Studies* 26 437-452
- Mandelbrot B B, 1983 *The Fractal Geometry of Nature* (W H Freeman, San Francisco, CA)
- Martin D J, 1991 *Geographic Information Systems and their Socioeconomic Applications* (Routledge, London)
- Maselli F C, Conese L, Petkov L, Resti R, 1992, "Inclusion of prior probabilities derived from a nonparametric process in the maximum likelihood classifier" *Photogrammetric Engineering and Remote Sensing* 58 201-207
- Mesev T V, 1992, "Integration between remotely sensed images and population surface models", paper presented to the Regional Science Association, University of Dundee, Scotland, 15-18 September; copy available from author
- Mesev T V, 1993, "Population prior probabilities in urban image classification", paper presented at the Annual Meeting of the Association of American Geographers, Atlanta, GA, 6-10 April; copy available from author
- Openshaw S, 1984 *Concepts and Techniques in Modern Geography, 38: The Modifiable Areal Unit Problem* (Geo Books, Norwich)
- Sadler G J, Barnsley M F, 1990, "Use of population density data to improve classification accuracies in remotely-sensed images of urban areas", working report 22, South East Regional Research Laboratory, Birkbeck College, London
- Skidmore A K, Turner B J, 1988, "Forest mapping accuracies are improved using a supervised nonparametric classifier with SPOT data" *Photogrammetric Engineering and Remote Sensing* 54 1415-1421
- Strahler A H, 1980, "The use of prior probabilities in maximum likelihood classification of remotely sensed data" *Remote Sensing of Environment* 10 135-163
- Vicsek T, 1989 *Fractal Growth Phenomena* (World Scientific, Singapore)